Selection of charged-current neutrino-induced K^+ production interactions in MicroBooNE

MICROBOONE-NOTE-1071-PUB

The MicroBooNE Collaboration

MICROBOONE_INFO@fnal.gov

June 2020

Abstract

MicroBooNE is an 85-ton active mass liquid-argon time projection chamber (LArTPC) neutrino detector exposed to the Booster Neutrino Beam (BNB) at Fermilab. MicroBooNE's physics goals is the precision measurement of neutrino interactions on argon in the 1 GeV energy regime. The study of neutrino interactions producing a K^+ in the final-state can improve the background estimates for future proton-decay experiments looking for the $p \to K^+\nu$ channel on argon such as DUNE. In this document we present a simulation study for a selection of events with a K^+ that is produced in a charged-current neutrino interaction and decays into a μ^+ and a ν_μ in the MicroBooNE detector. It will focus on how we use the particle identification techniques developed by MicroBooNE to achieve a sample with a 7% efficiency and 66.7% purity. This is the first step toward a charged-current kaon production cross section measurement in argon.

1 Motivation

The observation of neutrino-induced K^+ production in argon is of primary importance to understand backgrounds from atmospheric neutrino interactions in rare proton-decay searches looking for the $p \to K^+\nu$ channel in multi-kton liquid-argon (LArTPC) experiments such as DUNE. A few events of this particular production mode have been experimentally observed, and available measurements are only on light nuclear targets such as deuterium, neon, and carbon. So far there are no measurements on argon or any other nuclear target in the 1 GeV neutrino energy regime.

MicroBooNE [1] is a large LArTPC exposed to the Booster Neutrino Beam (BNB) at Fermilab and has collected a high statistics sample of neutrino interactions. Kaons produced by neutrino interactions in MicroBooNE have the same energy range as those produced by the proton-decay channel: $p \to K^+\nu$. Therefore, measurements of neutrino-induced kaons in MicroBooNE can improve the background estimates for future proton-decay searches by constraining the models of neutrino cross section of K^+ production in argon. They can also constraint models of K^+-argon interactions.

In this work we present a simulation study to estimate the efficiency and purity of selecting events with a K^+ that is produced in a charged-current neutrino interaction and decays into a μ^+ and a ν_μ in the MicroBooNE detector. The decay channel $K^+ \to \mu^+\nu_\mu$ is the dominant one and the μ^+ can be used to identify the parent K^+. This is a first step toward a charged-current kaon production cross section measurement in argon.

2 Neutrino-induced kaon production processes

Neutrino-induced kaon production can be observed in three forms:

- Associated kaon production: Produced kaon is accompanied by a hyperon in the final-state and strangeness is conserved after the interaction ($\Delta S = 0$). The neutrino energy threshold for this process is 1.1 GeV. See table 1 for a list of possible channels.

Charged-Current Mode	Neutral-Current Mode
$\nu_\mu + n \to \mu^- + K^+ + \Lambda^0$	$\nu_\mu + p \to \nu_\mu + K^+ + \Lambda^0$
$\nu_\mu + p \to \mu^- + K^+ + \Sigma^+$	$\nu_\mu + n \to \nu_\mu + K^0 + \Sigma^0$
$\nu_\mu + n \to \mu^- + K^+ + \Sigma^0$	$\nu_\mu + n \to \nu_\mu + K^+ + \Sigma^-$
$\nu_\mu + n \to \mu^- + K^0 + \Sigma^+$	$\nu_\mu + n \to \nu_\mu + K^- + \Sigma^+$

Table 1: Possible associated kaon production channels in both charged-current and neutral-current neutrino interactions.

- Single kaon production: Only one kaon is produced in the final-state and strangeness is not conserved after the interaction ($\Delta S = 1$). Even though the neutrino energy threshold for this process is lower than the associated production, at 0.8 GeV, it is suppressed due to the change of strangeness by a factor of $|V_{us}|^2 \approx 0.05$, where V_{us} is an element of the CKM matrix. See table 2 for a list of possible channels.

Charged-Current Mode
$\nu_\mu + p \rightarrow \mu^- + K^+ + p$
$\nu_\mu + n \rightarrow \mu^- + K^0 + p$
$\nu_\mu + n \rightarrow \mu^- + K^+ + n$

Table 2: Possible single kaon production channels in a neutrino charged-current interaction. There are no neutral current production channels for this particular process.

- Coherent kaon production: As in the single kaon production, only one kaon is produced in the final-state. In a coherent process, however, the target nucleus remains intact after the interaction. This process is extremely rare compared with the other kaon production processes.

The signal definition for this analysis will use only the associated production channel to avoid over-prediction of signal event rates, as described in section 3. Future improvements to the analysis will include adding a model of single kaon production. Expected event rates in the MicroBooNE detector for associated and single kaon production as a function of neutrino energy can be seen in figure 1. Coherent kaon production is not included in current neutrino interaction generators. However, this is not a concern due to its extremely small cross section.

3 Simulation

MicroBooNE uses GENIE [2] (Generates Events for Neutrino Interaction Experiments) version 3.0.6 tune G18_10a_02_11a to simulate neutrino interactions in the detector. The neutrino flux prediction from the Booster Neutrino Beamline (BNB) described in [3] is used as input.

This version of GENIE simulates neutrino-induced kaon production by both associated and single processes. By default only the associated kaon production is enabled and the single kaon production needs to be turned on manually. The associated kaon production can happen via both baryonic resonances (RES) and Deep Inelastic Scattering (DIS). Only the baryonic resonances with hadronic invariant mass $W < 1.7$ GeV are simulated using the Rein-Sehgal model [4]. As a result, only the reaction $K^+\Lambda$ is allowed via resonance. To simulate DIS processes, GENIE uses the Bodek-Yang model [5]. For K^+ production via DIS in the energy regime of 1.7 GeV $< W <$ 2.3 GeV, GENIE uses a hadronization model based on the parameterization of Koba-Nielsen-Olese (KNO) scaling [6]. The regime 2.3 GeV $< W <$ 3.0 GeV is governed by the AGKY model [7], while for $W >$ 3.0 GeV, PYTHIA 6 [8] is used. The free parameters in these hadronization models are tuned in such a way that they agree with the observations of strange particle production in the Big European Bubble Chamber (BEBC) [9] [10] [11] [12] and the Fermilab bubble chamber [13] [14]. Charged-current single kaon production in GENIE is modeled using a treatment due to Alam *et al.* [15].

Figure 1 shows the neutrino energy distribution of neutrino interactions in MicroBooNE predicted by the associated and single kaon production models in GENIE. In this analysis, we use only the associated kaon production model in GENIE because it has been tuned to external data. Enabling the induced single kaon production model may become the source of an over-prediction in the neutrino energy regions where the single and associated kaon production processes overlap. In the future, single kaon production processes will be added to the analysis, in such a way as not to lose the tuning to external data.

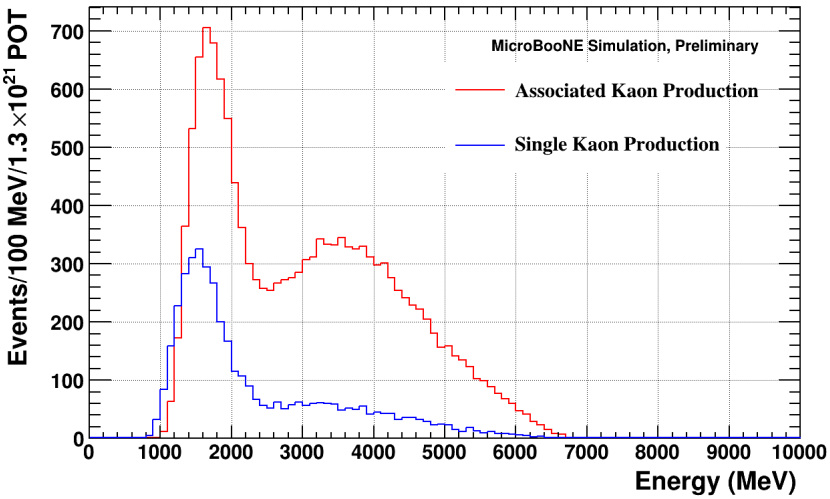

Figure 1: Neutrino energy distribution of single and associated kaon production predicted by GENIE 3.0.6 in the MicroBooNE detector. Here the two distributions are normalized to correspond to a beam exposure of 1.3×10^{21} protons on target (POT). The energy threshold of associated kaon production is 1.1 GeV while for single kaon production, it is 0.8 GeV.

To simulate hadronic final-state interactions, GENIE uses an effective cascade model named *hA*. This model only simulates inelastic scattering of kaons inside the nucleus. The result is a net loss of kinetic energy when the kaon emerges. A maximum of $\sim 5\%$ momentum loss due to final-state interaction of K^+ inside the argon nucleus was observed. K^+ production by charge exchange or pion interactions inside the nucleus is not simulated.

Once the particle emerges from the nucleus, GEANT4 (GEometry ANd Tracking) [16], [17] propagates the particles in several steps through the detector medium. In each step, GEANT4 decides whether the particle should hadronically interact, decay or (for charged particles only) continuously lose kinetic energy via ionization based on cross sections or decay lifetimes of the possible processes.

The full simulation used in this analysis is part of the current software framework developed by the MicroBooNE collaboration [18] [19] [20] [21] [22] [23]. The reconstruction of all types of particle tracks was done with the *Pandora* pattern-recognition framework [24].

Two simulated samples of neutrino interactions, where the simulated neutrino interaction is overlaid on a cosmic background event from data, were produced for this analysis. Both samples are listed in Table 3.

Sample name	POT
BNB	1.31×10^{21}
CCK	2.92×10^{23}

Table 3: The two Monte Carlo samples used in this analysis where the simulated neutrino interaction has been overlaid on a background cosmic event from data. The BNB sample contains all GENIE simulated neutrino interactions generated by GENIE 3.0.6 with the Booster Neutrino Beam flux while the CCK sample contains only events with one μ^- and one K^+ exiting the nucleus.

The purpose of the BNB sample is to estimate the rates of all types of interactions generated by GENIE 3.0.6 in the MicroBooNE detector with the Booster Neutrino Beam flux. In this sample, the number of charged-current interactions with a K^+ exiting the nucleus is expected to be very small ($\sim 0.1\%$) due to the small cross section with respect to other types of interactions. On the other hand, the CCK sample, which contains only events with a μ^- and K^+ exiting the nucleus, is used to have a larger sample of these kind of interactions to estimate signal efficiencies with much better statistics.

4 Signal definition

The goal of this analysis is to search for K^+ induced by ν_μ charged-current interactions (CC K^+) in the MicroBooNE detector. This K^+ can interact inside the detector producing several other particles, or they can decay with the decay products playing a vital role in identifying the parent K^+. Table 4 summarizes the branching fractions of the most dominant K^+ decay modes.

Decay Mode	Branching Fraction (%)
$K^+ \to \mu^+ + \nu_\mu$	63.56
$K^+ \to \pi^+ + \pi^0$	20.67
$K^+ \to \pi^+ + \pi^+ + \pi^-$	5.583
$K^+ \to \pi^0 + e^+ + \nu_e$	5.07
$K^+ \to \pi^0 + \mu^+ + \nu_\mu$	3.352
$K^+ \to \pi^+ + \pi^0 + \pi^0$	1.760

Table 4: The six most dominant K^+ decay modes and branching fractions [25].

The first and second decay modes in table 4 are of particular interest because they are the most dominant. Both also involve two-body decays where the μ^+ or π^+ from the decay has a well-defined kinetic energy (and thus track length). These observations are helpful in mitigating backgrounds when selecting K^+.

Table 5 shows the predicted production rates of CC K^+ events in the MicroBooNE detector. The fiducial volume (FV) for neutrino interactions and K^+ containment is defined as the volume within the TPC 10 cm away from the edges of the TPC, except for the downstream edge which is 50 cm away. The FV dimensions are:

- $0 \text{ cm} < X < 246.35 \text{ cm}$
- $-106.5 \text{ cm} < Y < 106.5 \text{ cm}$
- $10 \text{ cm} < Z < 986.8 \text{ cm}$

For the decay μ^+ or π^+ containment, we consider a decay-FV defined as the volume within the TPC 5 cm away from all the edges. This volume is bigger than the FV to include events where the K^+ decays near the limits of the FV and the decay products extend outside it. The dimensions of this volume are:

- $5 \text{ cm} < X < 251.35 \text{ cm}$
- $-111.5 \text{ cm} < Y < 111.5 \text{ cm}$
- $5 \text{ cm} < Z < 1031.8 \text{ cm}$

The CCK sample has been scaled so that the number of events with a K^+ in the FV is the same as in the BNB sample. The scale factor is $SF = 353/83036 = 0.0042512$. This normalization allows us to estimate the rate of CC K^+ interactions for $1.31 \times 10^2 1$ POT in the CCK sample with better statistics than in the BNB sample. All CCK sample distributions shown in this document have been scaled to the BNB sample in this way.

Signal Type	BNB sample (events/1.31×10^{21} POT)	CCK sample (generated events)	CCK sample (events/1.31×10^{21} POT)
CC K^+ in fiducial volume	353	83036	353.0
CC K^+ (K^+ contained)	304	72279	307.3
CC K^+ all decays (K^+ contained)	193	46164	196.2
CC $K^+ \to \mu^+ + \nu_\mu$ (K^+ contained)	128	29360	124.8
CC $K^+ \to \pi^+ + \pi^0$ (K^+ contained)	40	9463	40.2
CC $K^+ \to \mu^+ + \nu_\mu$ (K^+ and μ^+ contained)	**103**	**23485**	**99.8**
CC $K^+ \to \pi^+ + \pi^0$ (K^+ and π^+ contained)	38	8849	37.6

Table 5: Expected number of events for different types of ν_μ charged-current interactions with a K^+ exiting the nucleus predicted by GENIE 3.0.6 in the MicroBooNE detector. The signal definition corresponds to the sixth row (in red) which includes all CC K^+ interactions where the K^+ is contained in the detector and decays into μ^+ and a ν_μ, with the μ^+ also being contained in the detector.

Distributions of the neutrino energy and K^+ kinematic variables computed using the CCK sample where the K^+ and decay μ^+ or π^+ are contained in the detector are shown in figure 2. Additional kinematic distributions for the decay μ^+ or π^+ are shown in figure 3. Note the two peaks in the kinetic energy and track lengths distribution of μ^+ or π^+ coming from the K^+ two-body decay at rest.

For this analysis, we define our signal as all ν_μ charged-current interactions in GENIE with:

- A K^+ created by associated production, because it is the production process tuned to external data in GENIE.
- The K^+ decays into a μ^+ and a ν_μ, because it is the most dominant decay channel and a two-body decay involving a μ^+ that permits separation from other decays.
- Both the K^+ and the decay μ^+ are fully contained in the detector.

This definition corresponds to the sixth row in table 5 where 103 (99.8) events are expected in the BNB (CCK) sample. Future versions will include K^+ two-body decays into π^+ adding 38 (37.6) events in the BNB (CCK) sample in our signal definition.

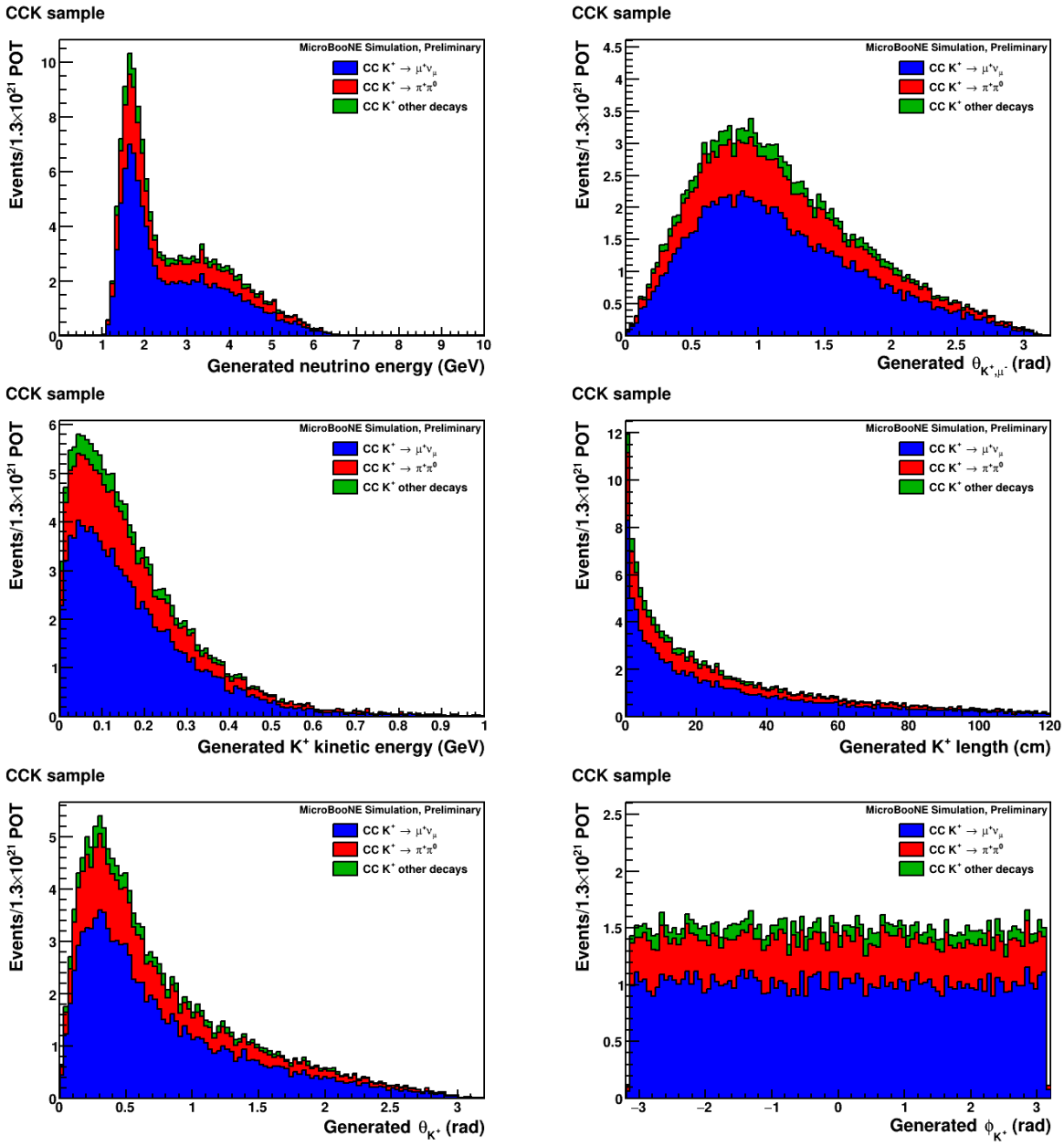

Figure 2: Distributions for CC K^+ interactions where the K^+ is produced by associated production and decays into a contained μ^+ or π^+ according to GENIE 3.0.6. Each histogram represents a distinct type of decay at the end of the K^+. The first two categories are the two-body K^+ decay to a μ^+ and π^+ respectively, and the third category consists of other K^+ decays to a μ^+ or π^+ (three-body decays). The different angles are defined as follows: θ_{K^+} is the angle between the K^+ and the neutrino beam direction, θ_{K^+,μ^-} is the angle between the K^+ and the μ^- from the charged-current interaction, and ϕ_{K^+} is the azimuthal angle around the neutrino beam direction.

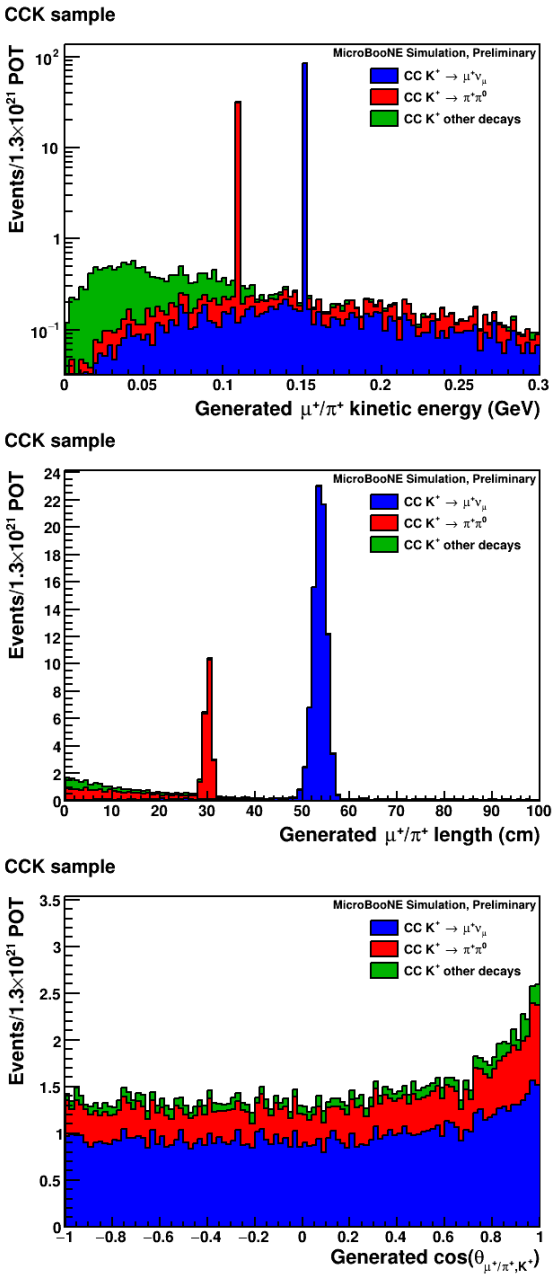

Figure 3: Distributions of generated μ^+ or π^+ from K^+ decay produced in CC K^+ events in the CCK sample. The variable $\theta_{\mu^+/\pi^+,K^+}$ is the angle between the decay μ^+/π^+ and the K^+.

5 Event Selection

In order to select signal interactions (CC $K^+ \to \mu^+$ with the K^+ and decay μ^+ contained in the detector), we apply a set of selection requirements on the event samples listed in table 3. Since the BNB sample contains only a few events with a K^+ exiting the nucleus, we use the CCK sample to better estimate the number of signal events throughout the selection.

The selection starts by requiring the event to pass a CC inclusive pre-selection. The pre-selection identifies neutrino- or cosmic-induced activity in an event using optical (prompt scintillation light) and topological (*Pandora* [24]) information. It selects the likely neutrino induced activity and uses PID and track length to identify a neutrino induced μ^- in the final-state. The number of signal events after the CC inclusive pre-selection in the BNB (CCK) sample is 46 (46.1) events, with a signal efficiency of 44.7% (46.2%). The signal purity in the BNB sample is 0.03%.

We then count the number of tracks associated with the reconstructed neutrino interaction vertex and accept events with 2 or more tracks. One track is the reconstructed μ^- from the charged-current interaction and the others are considered potential K^+ candidates. The number of signal events after this requirement in the BNB (CCK) sample is 45 (44.8), with a signal efficiency of 43.7% (44.9%). The signal purity in the BNB sample is 0.04%.

5.1 K^+ candidate selection

We search for K^+ candidates from all available tracks associated with the neutrino vertex but excluding the reconstructed μ^- identified by the CC inclusive pre-selection. First, we require the track to be contained in the detector. The start and end points of the track need to be inside the FV defined in section 4. Second, we use the particle identification based on energy loss per unit length (dE/dx).

When a charged particle traverses a medium the main source of energy loss is ionization. Moreover, ionization energy loss is strongly correlated with the particle's mass at low velocities for a given medium. Thus, if a given particle is known to come to rest before it undergoes any interaction other than ionization, then the dE/dx profile of that particle can be used as a tool to categorize its type.

The MicroBooNE detector consists of an homogeneous volume of liquid argon between a cathode plane at a voltage or -70 kV) and 3 different anode wire planes near ground voltage. The distance between the first anode wire plane and the cathode plane is 256 cm. The electrons produced when a charged particles ionize the liquid argon drift to the anode wire planes due to the electric field (273 V/m) between the cathode and anode wire planes. The ionization electrons induce a current in the wires of the first two planes and get collected by the third plane. The first two planes are called induction planes and the wires are oriented at $\pm 60°$ respect to the vertical direction. The third plane is called the collection plane and the wires are oriented vertically. The distance between all the wires in a plane is 3 mm. Signals recorded in the wires are used to determine the trajectory and dE/dx profile of the charged particle crossing the detector volume.

In MicroBooNE, we calculate a χ^2 value for each track under different particle hypotheses. The χ^2 value is obtained by comparing the dE/dx profile measured by the anode wire planes with standard dE/dx profiles for the particle hypothesis calculated using the Bethe-Bloch formula in liquid argon [26]. In this analysis, we use the χ^2 values under the kaon and proton hypotheses (χ^2_K and χ^2_P respectively) measured in the collection plane. Distributions of these values were generated for all contained tracks originated at the reconstructed

neutrino vertex but excluding the reconstructed μ^- identified by the CC inclusive pre-selection, and they are shown in figure 4. The generated particle associated with a track is the one that contributes the most energy to the hits belonging to that track. Tracks where $\chi^2_P > 4$ and $\chi^2_K < 15$ are accepted as K^+ candidates. It can be noted from figure 4 that the main challenge for this analysis is the high number of accepted proton tracks. Most other particles (pions and muons) are successfully rejected by this requirement.

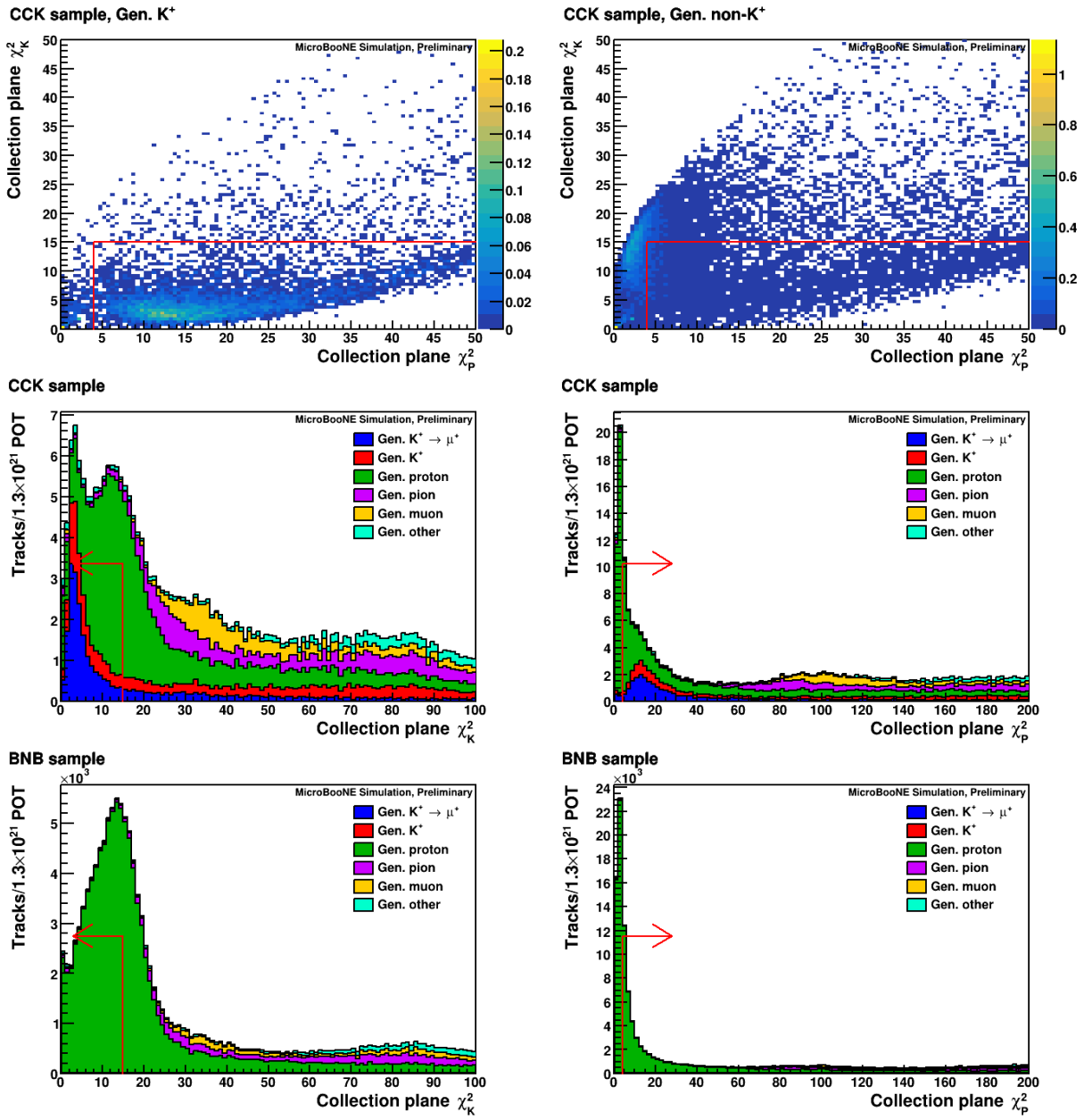

Figure 4: Distributions in the χ^2_P-χ^2_K phase space used for the K^+ candidate selection in the BNB and CCK samples. The legend shows the generated particle that produced the track. Red lines and arrows define the acceptance region.

The number of signal events with at least 1 K^+ candidate in the BNB (CCK) sample is 21 (19.9), with a signal efficiency of 20.4% (20.0%). The signal purity in the BNB sample is 0.08%.

5.2 μ^+ candidate selection

Proton tracks are the main background selecting K^+ candidates. Since they do not decay or interact producing a μ^+, to further improve the selection, we check if daughter tracks at the end of the K^+ candidate are compatible with a μ^+. First, we consider daughter tracks starting within 10 cm of the K^+ candidate end point and contained in the decay-FV defined in section 4. This volume is slightly bigger than the FV used for the K^+ candidates and allows daughter tracks to start at the edge of the FV and propagate outside it. Second, we generate distributions of the daughter track length, χ^2_P and distance to the K^+ candidate for all considered daughter tracks. Based on these distributions, shown in figure 5, we chose the following selection criteria:

- Daughter track distance to $K^+ < 5$ cm
- Daughter track length > 30 cm
- Daughter track $\chi^2_P > 50$

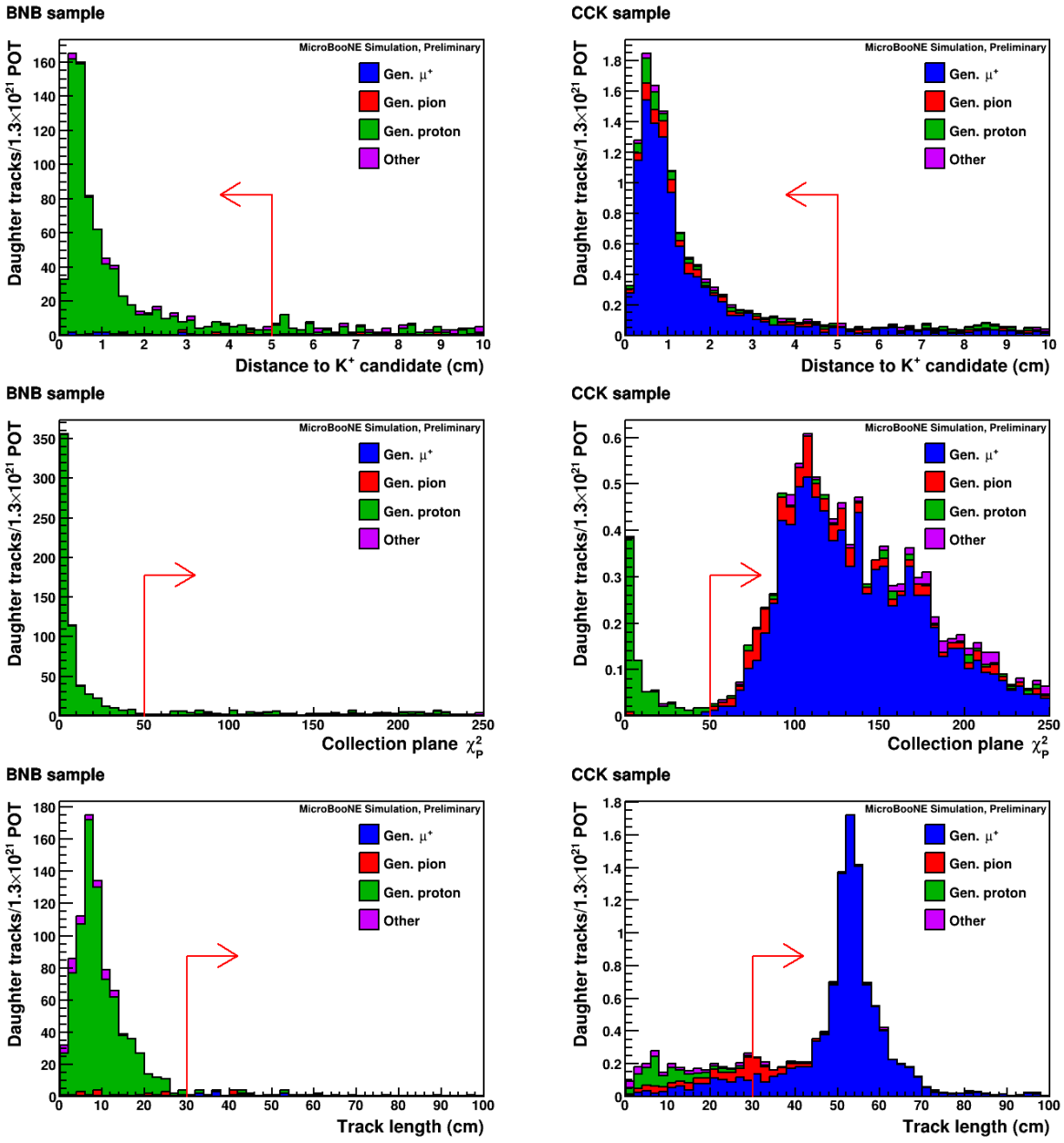

Figure 5: Distribution of variables used to select μ^+ candidates from tracks within 10 cm of the K^+ candidate end point for the BNB (left) and CCK (right) samples. Tracks with the distance to the K^+ candidate < 5 cm, length > 5 cm and $\chi^2_P > 50$ are selected as μ^+ candidates. The legend shows the generated particle that produced the track. Red lines and arrows define the acceptance region.

5.3 K^+ candidate with a μ^+ candidate

The distribution of the number of K^+ candidates with a μ^+ candidate for the CCK and BNB sample are shown in figure 6. We select events having exactly 1 K^+ candidate with a μ^+ candidate. The number of signal events after this requirement in the BNB (CCK) sample is 8 (7.01), with a signal efficiency of 7.77% (7.02%). The signal purity in the BNB sample is 66.7%.

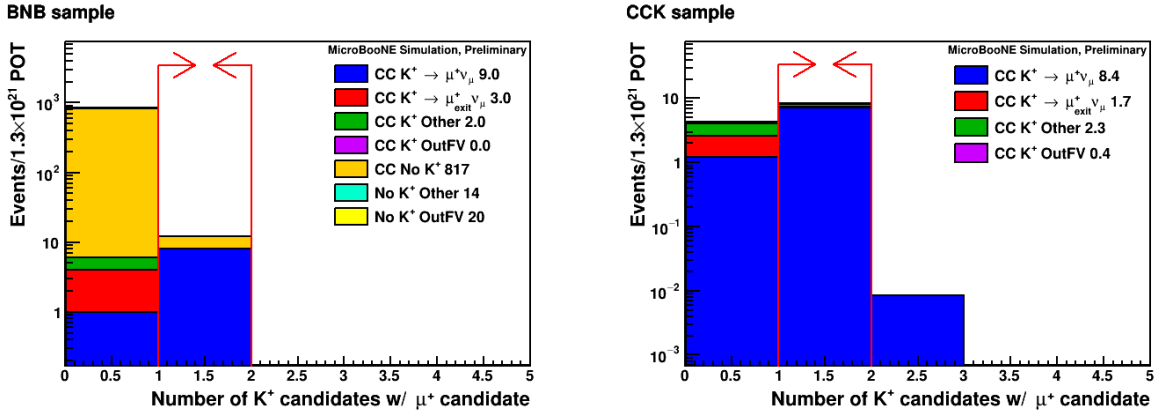

Figure 6: Number of K^+ candidates with a μ^+ candidate distributions for the BNB (left) and CCK (right) samples. Events with exactly 1 K^+ candidate with a μ^+ candidate are accepted. Red lines and arrows define the acceptance region.

6 Results

We have described an event selection to isolate charged-current neutrino-induced K^+ which decay into a μ^+ and a ν_μ. A summary of the number of events passing the different selection requirements for the BNB and CCK samples is shown in table 6. Only 12 events passed all the selection requirements in the BNB sample with only 4 background events. Distributions of selected events as a function of generated variables for the CCK sample are shown in figure 7.

Selection criteria	BNB (total)	BNB (signal)	CCK (total)	CCK (signal)	E□. (%)	Purity (%)
0) All events	1042798	103	444.0	99.8	100.0	0.01
1) CC inclusive pre-selection	153425	46	147.7	46.1	46.2	0.03
2) Track multiplicity >= 2	124505	45	142.7	44.8	44.9	0.04
3) # of K^+ cand. >= 1	25641	21	47.92	19.9	20.0	0.08
4) # of K^+ cand. w/ μ^+ cand.=1	12	8	8.36	7.01	7.02	66.7

Table 6: Summary of the number of events after each selection criteria in the BNB and CCK samples. The signal corresponds to CC K^+ interactions where the K^+ is produced by associated production and decays into a μ^+ and a ν_μ, and the K^+ and μ^+ are contained in the detector. These estimates correspond to 1.31×10^{21} POT. Efficiencies are calculated using the number of signal events in the CCK sample and purities using the number of events in the BNB sample.

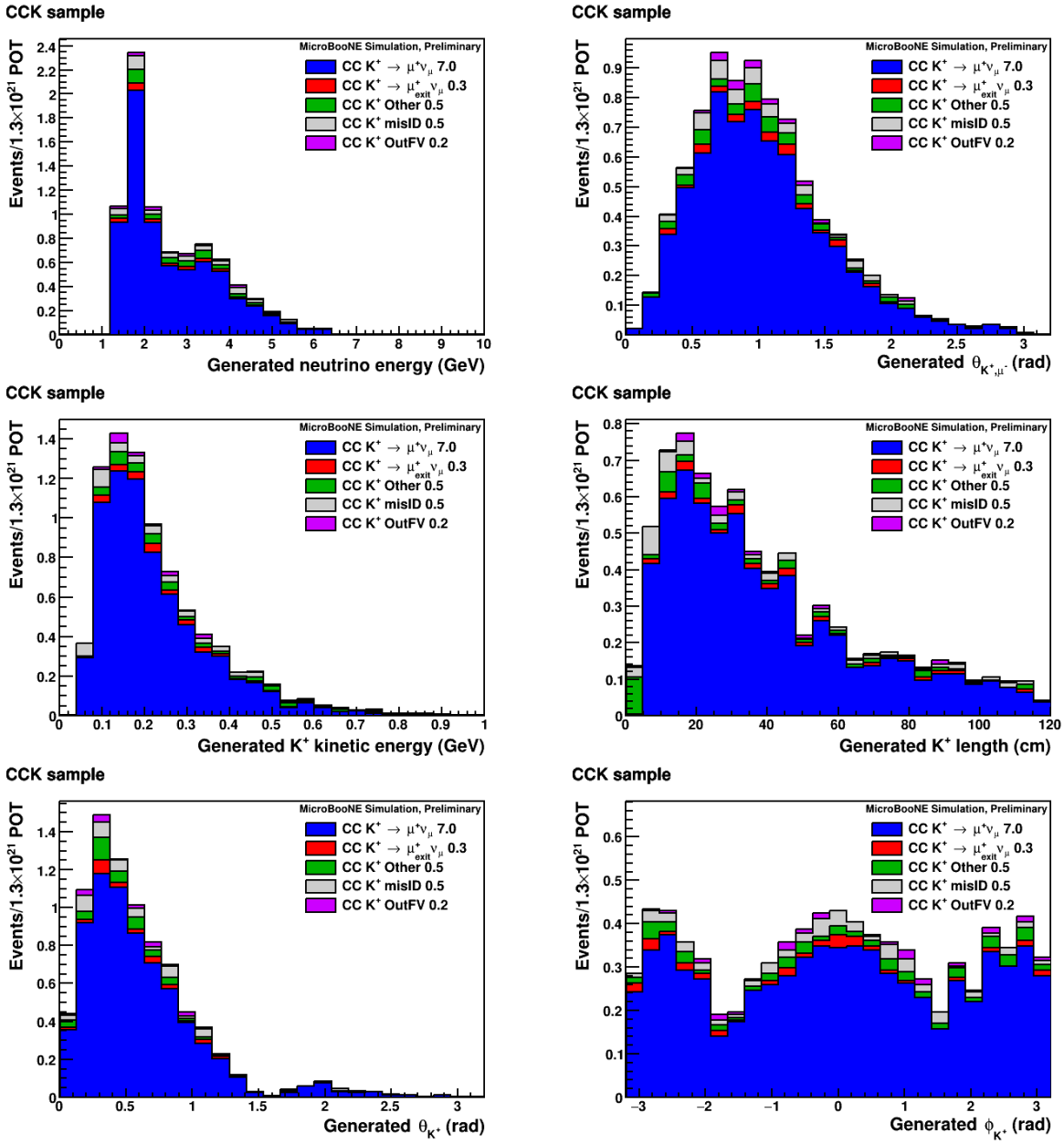

Figure 7: Selected events in the CCK sample as a function of generated variables. The "$CC\,K^+ \to \mu^+\nu_\mu$" category represents selected signal events. All the other categories are considered backgrounds with a K^+ in the final-state: If the μ^+ exits the detector, the event is in the "$CC\,K^+ \to \mu^+_{exit}\nu_\mu$" category; If the K^+ interacts or decays into other particles, it is in the "$CC\,K^+ \to Other$" category; If the K^+ or μ^+ candidate is not a generated K^+ or μ^+, it is in the "$CC\,K^+\,misID$" category; and if the K^+ is not contained in the detector, it is in the "$CC\,K^+\,OutFV$" category. The different angles are defined as follows: θ_{K^+} is the angle between the K^+ and the neutrino beam direction, θ_{K^+,μ^-} is the angle between the K^+ and the μ^- from the charged-current interaction, and ϕ_{K^+} is the azimuthal angle around the neutrino beam direction.

Also included in table 6 are the efficiency and purity after each requirement in the event selection. The efficiency is calculated using equation 1 applied to the CCK sample since it has better statistics of signal events. The efficiency denominator is populated with events in the signal definition described in section 4. The efficiency as a function of generated variable is shown in figure 8. The purity is calculated using equation 2 applied to the BNB sample because it includes all types of backgrounds. Due to the small number of events after all requirements in the BNB samples is not possible to plot the purity as a function of generated variables. The overall efficiency and purity of this event selection is 7.02% and is 66.7% respectively.

$$Efficiency = \frac{Selected\ CCK^+ \to \mu^+\ events}{Generated\ CCK^+ \to \mu^+\ events} \tag{1}$$

$$Purity = \frac{Selected\ CCK^+ \to \mu^+\ events}{Selected\ events} \tag{2}$$

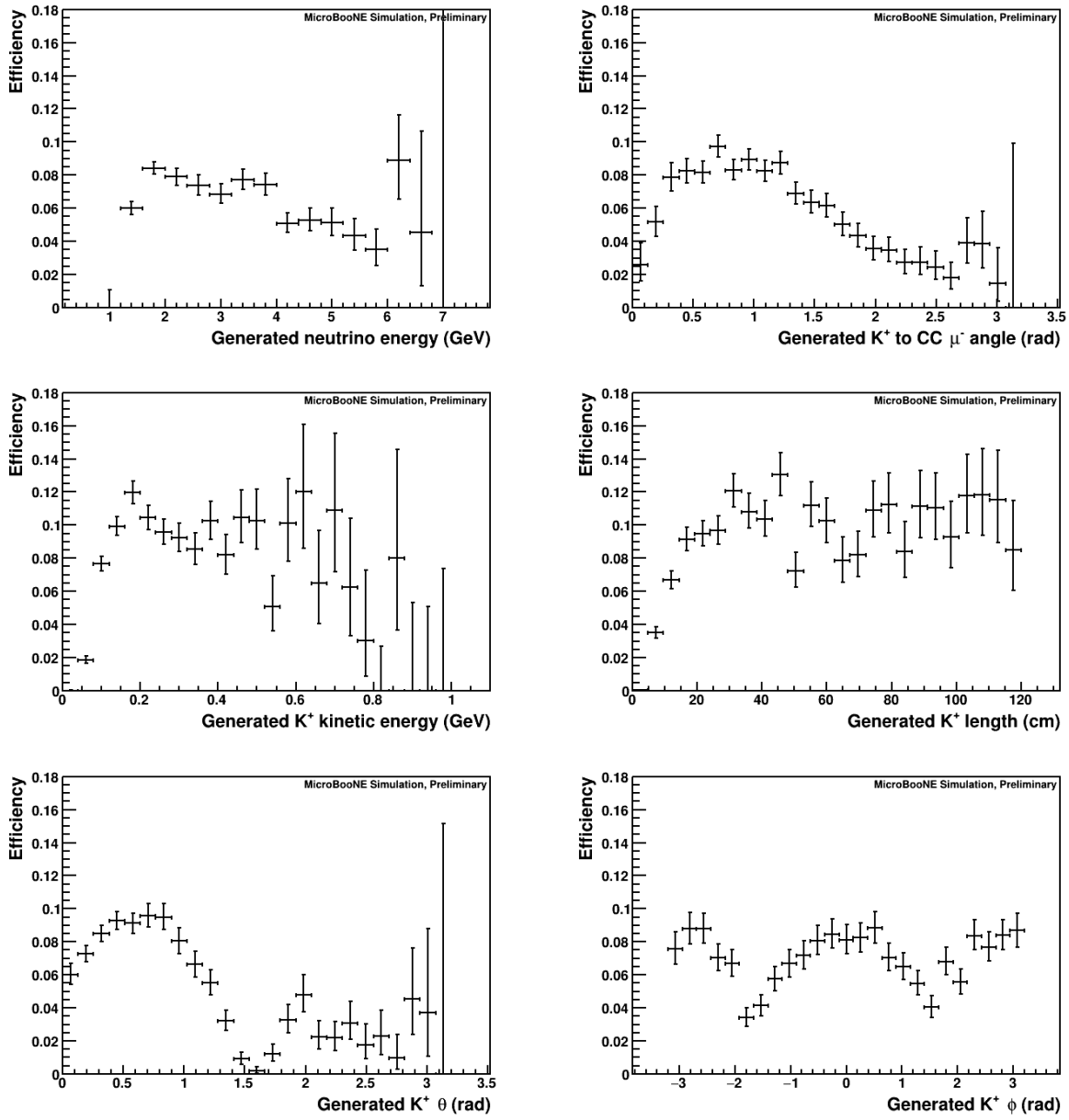

Figure 8: Event selection efficiency as a function of generated variables. The efficiencies where estimated from the CCK sample. Uncertainties are calculated using a Bayesian approach, reporting the 68% credible interval for a binomial process with uniform prior.

7 Selected candidate events

A list of the 12 CC $K^+ \to \mu^+\nu_\mu$ candidate events found in the BNB sample along with some information from GENIE is presented in table 7. The first 8 candidates (# 1-8) are signal events and the last 4 candidates (# 9-12) are background events. All background events in the BNB sample have a primary proton exiting the nucleus that has been misidentified as a K^+. This proton interacts inside the detector producing a secondary proton (candidate # 10) or pion (candidates # 9, 11 and 12) that are misidentified as a μ^+. Candidate # 1 is a signal event and it can be seen in the event display shown in figures 9. Candidate # 10 is a background event and it can be seen in the event display shown in figure 10.

Cand. #	Interaction	K^+ cand. gen. particle	decay μ^+ cand. gen. particle
1	CC RES, ν_μ Ar $\to \mu^-$ Λ^0 K^+ n 2p	K^+	μ^+
2	CC RES, ν_μ Ar $\to \mu^-$ Λ^0 K^+	K^+	μ^+
3	CC DIS, ν_μ Ar $\to \mu^-$ Σ^+ K^+ π^+ π^-	K^+	μ^+
4	CC DIS, ν_μ Ar $\to \mu^-$ Σ^+ K^+ π^+ n	K^+	μ^+
5	CC RES, ν_μ Ar $\to \mu^-$ Σ^+ K^+ n	K^+	μ^+
6	CC DIS, ν_μ Ar $\to \mu^-$ Λ^0 K^+ p	K^+	μ^+
7	CC DIS, ν_μ Ar $\to \mu^-$ Λ^0 K^+ n p	K^+	μ^+
8	CC RES, ν_μ Ar $\to \mu^-$ Λ^0 K^+	K^+	μ^+
9	CC RES, ν_μ Ar $\to \mu^-$ π^+ p	proton	π^+
10	CC MEC, ν_μ Ar $\to \mu^-$ 2n 2p	proton	proton
11	CC RES, ν_μ Ar $\to \mu^-$ π^+ 3p 2n	proton	π^+
12	CC RES, ν_μ Ar $\to \mu^-$ π^+ π^- π^0 n p	proton	π^+

Table 7: Selected CC $K^+ \to \mu + \nu_\mu$ candidate events found in the BNB sample. The first 8 candidates are signal events and the last 4 are background events.

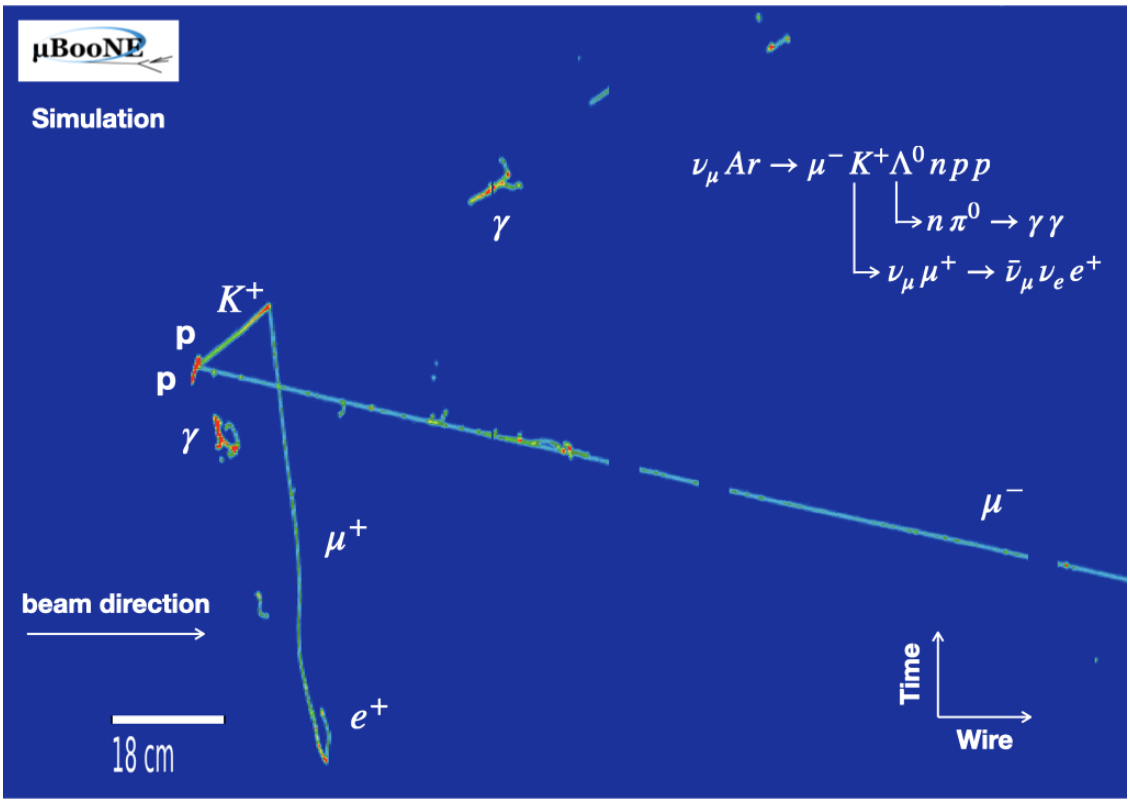

Figure 9: Event display (collection plane) for CC $K^+ \to \mu^+\nu_\mu$ candidate # 1 which is a signal event. The white labels represent the generated particles. The μ^-, K^+ and $\mu+$ have been correctly identified by the event selection.

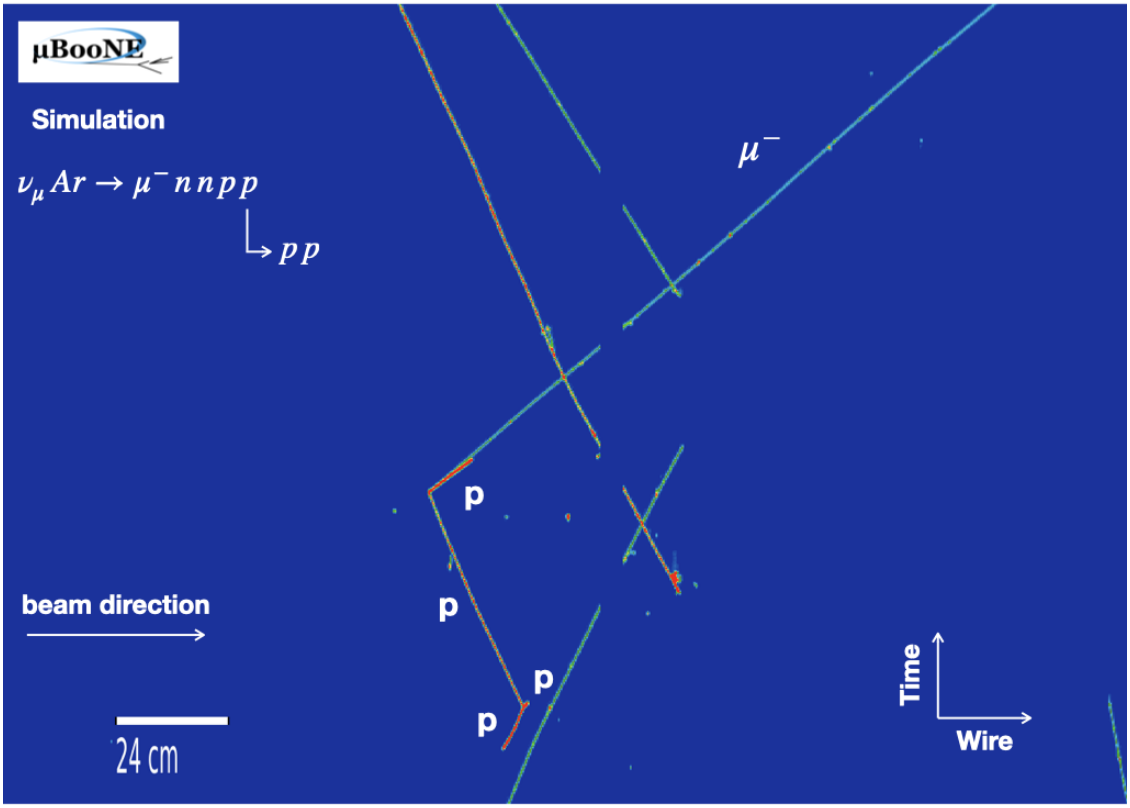

Figure 10: Event displays (collection plane) for CC $K^+ \rightarrow \mu + \nu_\mu$ candidate # 10 which is a background event. The white labels represent the generated particles producing the reconstructed track. The generated charged-current μ^- has been correctly identified. However, a generated proton producing another proton by an inelastic interaction has been mis-identified as a K^+ decaying into a μ^+ by the event selection.

8 Conclusions

We have described an event selection for charged-current neutrino-induced K^+ production where the K^+ decays into a μ^+ and a ν_μ with an overall efficiency of 7.02% and a purity of 66.7%. This is a simulation only study and the first step toward a charged-current kaon production cross section measurement in argon. Future versions of this selection will include the single K^+ production process in the simulation and other K^+ decay modes, such as $K^+ \to \pi^0\pi^+$, to improve efficiency.

References

[1] R. Acciarri et al. (MicroBooNE Collaboration).“Design and Construction of the MicroBooNE Detector.” JINST 12 P02017, 2017. DOI: 10.1088/1748-0221/12/02/P02017.

[2] C.Andreopoulos *et al.*, Nucl. Instr. Meth. A 614, 87 (2010).

[3] MicroBooNE collaboration, “Booster Neutrino Flux Prediction at MicroBooNE”, MICROBOONE-NOTE-1031-PUB.

[4] D. Rein and L. M. Sehgal, Annals Phys. 133, 79 (1981).

[5] A. Bodek, I. Park and U.-K. Yang, Nucl. Phys. Proc. Suppl. 139, 113 (2005).

[6] Z. Koba, H. B. Nielsen, and P. Olesen, Nucl. Phys. B 40, 317 (1972).

[7] T. Yang *et al.*, Eur. Phys. J. C 63, 1 (2009).

[8] T. Sjostrand, S. Mrenna and P. Skands, JHEP 05, 26 (2006).

[9] G.T. Jones et al., Z. Phys. C 57, 197 (1993).

[10] D. Allasia et al., Nucl. Phys. B 224, 1 (1983)

[11] P. Bosetti et al., Nucl. Phys. B 209, 28 (1982).

[12] S. Willocq et al., Z. Phys. C 53, 207 (1992).

[13] N.J. Baker et al., Phys. Rev. D 34, 1251 (1986).

[14] D. DeProspo et al., Phys. Rev. D 50, 6691 (1994).

[15] M. Alam *et al.*, Phys. Rev. D 82, 033001 (2010).

[16] S. Agostinelli *et al.*, Nuc. Instr. Meth. A 506, 250 (2003).

[17] J. Allison *et al.*, IEEE Trans. Nuc. Sci. 53 No. 1, 270 (2006).

[18] MicroBooNE collaboration, “Noise Characterization and Filtering in the MicroBooNE Liquid Argon TPC”, JINST 12, P08003 (2017).

[19] MicroBooNE collaboration, "Ionization Electron Signal Processing in Single Phase LAr TPCs I: Algorithm Description and Quantitative Evaluation with MicroBooNE Simulation", JINST 13, P07006 (2018).

[20] MicroBooNE collaboration, "Ionization Electron Signal Processing in Single Phase LAr TPCs II: Data/Simulation Comparison and Performance in MicroBooNE", JINST 13, P07007 (2018).

[21] MicroBooNE collaboration, "Calibration of the Charge and Energy Response of the MicroBooNE Liquid Argon Time Projection Chamber Using Muons and Protons", JINST 15, P03022 (2020).

[22] MicroBooNE collaboration, "A Method to Determine the Electric Field of Liquid Argon Time Projection Chambers Using a UV Laser System and its Application in MicroBooNE", arXiv:1910.01430, submitted to JINST.

[23] MicroBooNE collaboration, "Study of Space Charge Effects in MicroBooNE", MICROBOONE-NOTE-1018-PUB.

[24] MicroBooNE collaboration, "The Pandora Multi-Algorithm Approach to Automated Pattern Recognition of Cosmic Ray Muon and Neutrino Events in the MicroBooNE Detector", Eur. Phys. J. C78, 1, 82 (2018).

[25] M. Tanabashi et al. (Particle Data Group), Phys. Rev. D 98, 030001 (2018).

[26] MicroBooNE collaboration, "Detector calibration using through going and stopping muons in the MicroBooNE LArTPC", MICROBOONE-NOTE-1048-PUB.